

impressions arose at the inner surface of the shaft, i.e., traces of the pressure of the wedges. The identity (visual) of the impressions bears witness to the uniformity of the distribution of the stresses.

In another model, a piston with a diameter of 50 mm was used, having values of  $\lambda$ ,  $\gamma$ , and  $\beta$  equal approximately to 0.9, 0.87, and 0.45, respectively. The working pressure of the compressed gas was around 2000 atm. The maximal radial stresses in this case, according to the calculation, around 1200 atm.

It must be noted that, in several hundreds of cycles of work, there was no case of breakdown of the system or of damage to its elements.

#### LITERATURE CITED

1. Von Karman Institute for Fluid Dynamics, Education, and Research, 1956-1976 (1976).
2. A. A. Meshcheryakov and V. I. Pinakov, "The piston of an adiabatic compression device," Inventor's Certificate No. 390315, Byull. Otkr., Izobr., Prom. Obraz., Tov. Znaki, No. 30 (1973).
3. S. D. Ponomarev et al., Strength Calculations in Machine Building [in Russian], Vol. 2, Mashgiz, Moscow (1958).

#### ANALYSIS OF STRUCTURE ELEMENTS TAKING ACCOUNT OF MATERIAL DAMAGE DURING CREEP

V. A. Zaev and A. F. Nikitenko

UDC 539.376

Deformations accumulated in the third stage of creep [1, 2] are neglected in the analysis of structure elements in the majority of cases. However, as follows from an analysis of experimental results [3], some structural materials disclose quite definite third sections of creep even for insignificant deformations on the order of 1-2%.

A standard computation of the stress-strain state for this scheme and the strength analysis of the structure elements under creep conditions do not take account of the fact [1] that cumulative damage, which exerts substantial influence on the creep rate and results in redistribution of the stress field, precedes fracture.

An analysis of vessels stressed by internal pressure is presented below, in which the circumstances noted above are taken entirely into account. The stress-strain state of the vessels and the lower boundary of the fracture time are determined. It is noted that the elucidated method of solution is simpler and more effective in the volume and complexity of the calculational procedures than the traditional methods [1].

Let a uniformly heated vessel (sphere, cylinder) be loaded by a constant internal pressure  $p$  with respect to time. The equilibrium equations and boundary conditions have the form [1, 2]

$$\partial\sigma_r/\partial r + k(\sigma_r - \sigma_\varphi)/r = 0, \quad a \leq r \leq b; \quad (1)$$

$$\sigma_r(a) = -p, \quad \sigma_r(b) = 0, \quad (2)$$

where  $a$  and  $b$  are the inner and outer radii, respectively. For a cylindrical vessel  $k=1$ , while  $k=2$  for a spherical vessel, and  $\sigma_r$ ,  $\sigma_\varphi$  are the principal stress tensor components, which are functions of the time and the coordinate  $r$ . The remaining principal stress  $\sigma_\theta$  equals  $\sigma_\varphi$  [2] for a spherical vessel in the case of central symmetry, and  $\sigma_z$  for a cylindrical vessel is determined from the standard assumption about no creep in the axial direction [1, 2].

The creep strain rate tensor components are related to the displacement velocity vector components by the known Cauchy relations [2], while the equation of continuity of the creep strain rate has the form [2]

$$\partial\eta_\varphi/\partial r + (\eta_\varphi - \eta_r)/r = 0. \quad (3)$$

We write the system of equations describing all three stages of material creep and taking account of the damage process in time in the form [1, 4]

---

Novosibirsk. Translated from Zhurnal Prikladnoi Mekhaniki i Tekhnicheskoi Fiziki, No. 2, pp. 157-164, March-April, 1980. Original article submitted June 19, 1979.

$$\eta_j = \frac{\partial \Phi_1 / \partial \sigma_j}{\mu^m (1 - \mu)^{\alpha/(\alpha+1)}}; \quad (4)$$

$$\mu = \left[ 1 - (\alpha + 1)(m + 1) \int_0^t \Phi_2 d\tau \right]^{1/(m+1)}, \quad (5)$$

where  $j=r, \varphi, z$  for a cylinder, and  $j=r, \varphi, \theta$  for a sphere. Here  $\Phi_1, \Phi_2$  are homogeneous functions in the stresses of degree  $(n+1)$  and  $(g+1)$  of the form  $\Phi_1 = B_1 S_2^{(n+1)/2}$ ,  $\Phi_2 = B_2 S_2^{(g+1)/2}$ ,  $S_2$  is the second invariant of the stress tensor deviator ( $S_2 = (1/6)[(\sigma_1 - \sigma_2)^2 + (\sigma_2 - \sigma_3)^2 + (\sigma_3 - \sigma_1)^2]$ ). The function  $\mu$  is related to the damage parameter  $\omega$  by the relationship

$$\omega = (1 - \mu)^{1/(\alpha+1)} \quad (6)$$

obtained by integrating the kinetic equation [1, 4]

$$d\omega/dt = \Phi_2/\omega^\alpha (1 - \omega^{\alpha+1})^m, \quad \omega(r, 0) = 0, \quad \omega(r_*, t_*) = 1,$$

where  $B_1, B_2, m, n, g, \alpha$  are material characteristics,  $t_*$  is the time of the beginning of fracture front propagation [1, 2] determined from (6) by using (5):

$$(\alpha + 1)(m + 1) \int_0^{t_*} \Phi_2 d\tau = 1. \quad (7)$$

The time  $t_*$  at which  $\omega=1$  first at a certain point  $r_*$  of the body, will be designated the lower boundary of the body (structure element) fracture time.

The system (1)-(7) permits computation of the stress-strain state of vessels loaded by internal pressure at any time and determination of the lower boundary of the fracture time.

We seek the solution of the problem formulated as

$$\sigma_j(r, t) = \sigma_j^0(r) f(r, t) + C(r, t); \quad (8)$$

$$v_j(r, t) = v_j^0(r) F(t), \quad (9)$$

where  $v_j$  are the displacement velocity vector components, and  $\sigma_j^0, v_j^0, f(r, t), C(r, t), F(t)$  are functions to be determined. The zero superscript on the appropriate functions denotes that these latter depend only on the coordinate  $r$ .

From (9) we have

$$\eta_j(r, t) = \eta_j^0 F(t). \quad (10)$$

We select the function  $f(r, t)$  from the condition that substituting (8), (10) in the coupling equation (4) the variables could then be separated. For example, setting

$$f = [\mu^m (1 - \mu)^{\alpha/(\alpha+1)} X(t)]^{1/n} \quad (11)$$

to the accuracy of an arbitrary function of the time, we obtain

$$\frac{\eta_j^0}{\partial \Phi_1^0 / \partial \sigma_j^0} = \frac{1}{F(t) X(t)} = \text{const.}$$

Taking the constant equal to one, we see that

$$F(t) X(t) = 1, \quad (12)$$

and the components  $\eta_j^0, \sigma_j^0$  satisfy the steady creep equations [1, 2]. The solution of the steady creep problem for the vessels under consideration which are loaded by the very same constant internal pressure in time will later be considered known [2].

Taking the above-mentioned into account, it can be seen that the field of displacement velocities (9) identically satisfies the Cauchy relations and the zero boundary conditions. The equation of continuity of the creep strain rate (3) is also satisfied.

Substituting the stress tensor components (8) into the equilibrium equation (1), and the boundary conditions (2), we see that they are satisfied if the function  $C(r, t)$  here satisfies the differential equation

$$\frac{\partial C}{\partial r} + \sigma_r^0 \frac{\partial f}{\partial r} = 0 \quad (13)$$

at any time with the boundary condition

$$C(a, t) = -p[1 - f(a, t)], \quad C(b, t) = 0. \quad (14)$$

The reason for the occurrence of two boundary conditions (14) for the differential equation (13) is perfectly evident. Taking into account that the principal stress vector  $\sigma_z$  equals the force of the internal pressure on the bottom of a tube (or the principal stress vector  $\sigma_\theta$  equals the internal pressure force on the surface of a hemisphere), by taking account of (8) it can be shown that the second boundary condition for (13) is satisfied identically.

Let us turn to a determination of the functions  $\mu(r, t)$  and  $X(t)$  in terms of which  $f(r, t)$  is expressed according to (11). Using the energy theorem [2], we have

$$\int_s T_j^0 v_j ds = \int_V \sigma_j^0 f(r, t) \eta_j^0 F(t) dV. \quad (15)$$

On the other hand, taking into account that  $v_j(r, t) = v_j^0 F(t)$ ,  $v_j^0$  are compatible with  $\eta_j^0$ , and the external loads  $T_j^0$  which are constant in time are in equilibrium with  $\sigma_j^0$ , we obtain

$$\int_s T_j^0 v_j ds = F(t) \int_V \sigma_j^0 \eta_j^0 dV. \quad (16)$$

We have from a comparison between (15) and (16)

$$\int_V f(r, t) \sigma_j^0 \eta_j^0 dV = \int_V \sigma_j^0 \eta_j^0 dV. \quad (17)$$

Taking into account that  $\sigma_j^0 \eta_j^0 = (n+1)\Phi_1^0$ , and applying the theorem of the mean to the first integral in (17)

$$\int_V f(r, t) \Phi_1^0 dV = \bar{f}(r(t), t) \int_V \Phi_1^0 dV, \quad (18)$$

we finally obtain that at any time the equality

$$\bar{f}(r(t), t) = 1, \quad 0 \leq t \leq t_*,$$

should be satisfied, which permits determination in combination with (11) of the time function  $X(t)$ :

$$X(t) = \bar{\mu}^m (1 - \bar{\mu})^{\alpha(\alpha+1)}, \quad \bar{\mu} = \mu(\bar{r}(t), t). \quad (19)$$

Substituting (8) into (5), we obtain after the simplest manipulations with (11) taken into account

$$\int_1^\mu z^\rho (1-z)^{-\rho} dz = -[(m+1)t_*^0]^{-1} \int_0^t X^{-(g+1)/n} d\tau, \quad (20)$$

and taking (11) into account we have from (17)

$$\int_V [\mu^m (1 - \mu)^{\alpha(\alpha+1)}]^{1/n} \Phi_1^0 dV = X^{1/n} \int_V \Phi_1^0 dV. \quad (21)$$

Here

$$l = \frac{m(n-g-1)}{n}; \quad \rho = \frac{\alpha}{\alpha+1} \frac{g+1}{n}; \quad t_*^0 = [(\alpha+1)(m+1)\Phi_1^0]^{-1}.$$

For the integration in (20) it must be taken into account that  $1 \geq \mu(r, t) > 0$  for  $0 \leq t < t_*$ ,  $\mu(r_*, t_*) = 1$ ,  $X(0) = 1$ ,  $X(t_*) > 0$ . This imposes certain constraints on the material characteristics which are not generally too strict.

It follows from the above that the problem (1)-(7) formulated above for creep theory with the material damage taken into account simultaneously can be reduced to a steady creep problem. In order to obtain the desired solution  $\sigma_j, \eta_j$  the known steady creep solution  $\sigma_j^0, \eta_j^0$  should be multiplied by the functions  $f(r, t)$  and  $F(t)$ , respectively. The hydrostatic component is found from the solution of the differential equation (13) and the boundary condition (14).

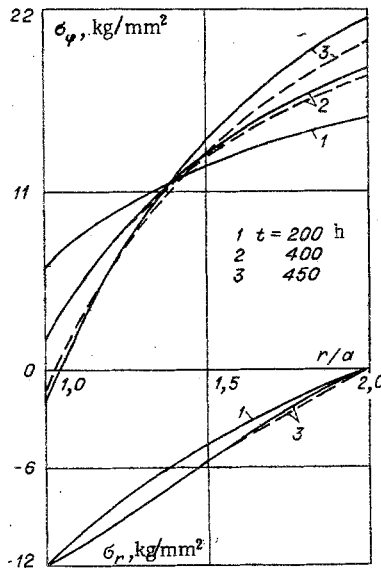


Fig. 1

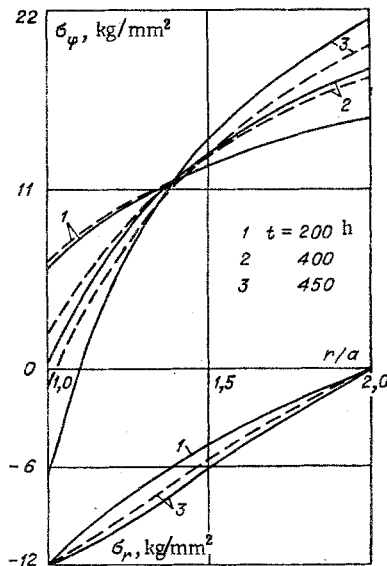


Fig. 2

One of the known numerical methods of solving the system (20), (21) is required to determine the functions  $f(r, t)$  and  $F(t)$  which are expressed in terms of  $\mu(r, t)$  and  $\bar{\mu}(t)$  according to (11) and (12).

Substituting (8) into (7), we find the lower bound of the fracture time, after which propagation of the fracture front starts from the point  $r = r_*$  as most stressed

$$\int_0^{t_*} [f(r_*, t)]^{s+1} dt = t_*^0(r_*). \quad (22)$$

Since the function  $f(r, t)$  is related to the damage parameter  $\omega(r, t)$ , it then follows from (8) that the latter exerts substantial influence on the stress field by contributing to its redistribution from the time of load application to the beginning of fracture. Evidently  $f(r, 0) = 1$ ,  $C(r, 0) = 0$ , and therefore, the stress field (8) agrees with the steady distribution  $\sigma_j^0$  for  $t = 0$ .

Limiting ourselves to the case of a material becoming soft during creep, i.e., when  $\alpha = 0$ , we determine  $\mu$  and  $\bar{\mu}$  from the system (20) and (21) as follows. Using the notation

$$\int_0^t \bar{\mu}^{-(m+1)\alpha} d\tau = u, \quad u(0) = 0, \quad \frac{du}{dt} = 1 \quad \text{for } t = 0,$$

$$\beta = m/(n + m(n - g - 1)), \quad \nu = (n + m(n - g - 1))/n(m + 1),$$

$$\alpha = m(g + 1)/n(m + 1), \quad \gamma = m/n(m + 1)$$

and substituting  $\mu(r, t)$  from (20) into (21), we obtain

$$\int_V \Phi_1^0 \left(1 - \frac{\nu}{t_*^0} u\right)^\beta dV = (du/dt)^{-\gamma/\alpha} \int_V \Phi_1^0 dV. \quad (23)$$

We seek the solution of (23) in the form of a power series in  $t$ :

$$u = \sum_{k=1}^{\infty} b_k t^k, \quad b_1 = 1.$$

Then we have for  $\mu(r, t)$  and  $\bar{\mu}(t)$

$$\mu^{m/n} = 1 + \sum_{k=1}^{\infty} B_k t^k; \quad (24)$$

$$\bar{\mu}^{m/n} = 1 + \sum_{k=1}^{\infty} D_k t^k, \quad (25)$$

where

$$B_k = \sum_{i=1}^k (-1)^i \frac{A_\beta^i}{i!} b_k^{(i)}; \quad b_k^{(i)} = \sum_{n=1}^{k-1} b_n^{(1)} b_{k-n}^{(i-1)};$$

$$b_k^{(i)} = 0 \quad \text{for } k < i, \quad i > 1; \quad b_k^{(1)} = (m+1) \Phi_2^0 \nu b_k;$$

$$D_k = \sum_{i=1}^k \frac{A_{(-\gamma/\alpha)}^i}{i!} d_k^{(i)}; \quad d_k^{(i)} = \sum_{n=1}^{k-1} d_n^{(1)} d_{k-n}^{(i-1)};$$

$$d_k^{(i)} = 0 \quad \text{for } k < i, \quad i > 1; \quad d_k^{(1)} = (k+1) b_{k+1};$$

$A_m^n$  is the number of permutations of  $m$  elements  $n$  at a time. After standard operations, we obtain a formula from which we determine the expansion coefficients  $B_k$  and  $D_k$ :

$$D_k \int_V \Phi_1^0 dV = \int_V \Phi_1^0 B_k dV.$$

Let us write down some of the first coefficients:

$$D_1 = -\beta\nu/t_*^0, \quad B_1 = -\beta\nu/t_*^0,$$

$$D_2 = \frac{(\beta\nu)^2}{2!} \left[ -\frac{\alpha}{\gamma} + \frac{(\beta-1)\lambda_1}{\beta} \right] \frac{1}{(t_*^0)^2},$$

$$B_2 = \frac{(\beta\nu)^2}{2!} \left[ -\frac{\alpha}{\gamma} \frac{t_*^0}{t_*^0} + \frac{\beta-1}{\beta} \right] \frac{1}{(t_*^0)^2},$$

where

$$\lambda_1 = \frac{\int_V \Phi_1^0 \Phi_2^{02} dV \int_V \Phi_1^0 dV}{\left( \int_V \Phi_1^0 \Phi_2^0 dV \right)^2},$$

and  $t_*^0$  is determined from the expression

$$t_*^0 = [(m+1) \Phi_2^0(\bar{r})]^{-1} = [(m+1) \bar{\Phi}_2^0]^{-1},$$

where

$$\bar{\Phi}_2^0 = \int_V \Phi_1^0 \Phi_2^0 dV / \int_V \Phi_1^0 dV. \quad (26)$$

Direct computations show that a perfectly good approximation can be obtained in determining the stress-strain state if the sums of the infinite series (24) and (25) are approximated by the expressions

$$\mu^{m/n} = \left\{ 1 + \frac{\bar{i}_*^0}{i_*^0} \left[ \left( 1 - \frac{t}{i_*^0} \right)^\nu - 1 \right] \right\}^\beta; \quad (27)$$

$$\bar{\mu}^{m/n} = \left( 1 - \frac{t}{i_*^0} \right)^\nu. \quad (28)$$

Diagrams of the stress distributions in a thick-walled tube at different times are represented by solid lines in Fig. 1. The computation was performed by means of the dependences (8) by using (27) and (28). The material characteristics had the values:  $\lambda = b/a = 2$ ,  $n = g = 4$ ,  $m = 3$ ,  $B_1 = 9.4 \cdot 10^{-9}$ ,  $\sigma_r(a) = -12 \text{ kg/mm}^2$ . Here the stress distribution diagrams obtained in a direct computation by using an electronic computer are represented by dashed lines for comparison. The time interval between 0 and  $t$  was here divided into bands  $\Delta t$  and the computation was performed by a standard method [1].

Substituting (27) and (28) into (22), we obtain the following expression:

$$t_* = \bar{i}_*^0 \left[ 1 - \left( 1 - i_*^0(a)/\bar{i}_*^0 \right)^{1/\nu} \right] \quad (29)$$

for the time of the beginning of fracture front propagation. In particular,  $t_*$  calculated from (29) was 473 h, but  $t_* = 488 \text{ h}$  in a direct computation. It is seen hence and from a comparison of the stress distribution diagrams represented in Fig. 1 that the method elucidated to compute the stress-strain state of high-pressure vessels and to determine the lower bound of the fracture time yields a perfectly good approximation to actuality. Evidently it is much simpler and more effective in the volume and complexity of the calculational procedures as compared with traditional methods [1, 2].

In the particular case when the material characteristics are associated with the relationship ( $\beta = 1$ )

$$m = n/(2 - (n - g)) \text{ for } 1 < n - g < 2, \\ m = n/2 \text{ for } n = g,$$

the system (20) and (21) has the simple solution

$$\mu_1^{m/n} = 1 + \frac{\bar{i}_*^0}{i_*^0} \left[ \left( 1 - \frac{t}{i_*^0} \right)^\nu - 1 \right]; \quad (30)$$

$$\bar{\mu}^{m/n} = \left( 1 - t/i_*^0 \right)^\nu. \quad (31)$$

This same result can be obtained directly from (24) and (25). The lower bound of the fracture time is determined from (29) by replacing  $\nu$  by  $\gamma$  ( $\nu = \gamma$  for  $\beta = 1$ ).

It turns out that in the case  $\beta \neq 1$  a perfectly satisfactory approximation can be obtained in the computation of the stress-strain state if the sums of the infinite series in (24) and (25) are approximated by (30) and (31). The appropriate stress distribution diagrams are represented by solid lines in Fig. 2 for different times computed by means of (8) by using (30) and (31) (the dashed lines are the same as in Fig. 1). The lower bound of the fracture time, as determined from (29) where  $\nu$  was replaced by  $\gamma$ , was 461 hrs.

Let us note that a lower bound in the fracture time  $t_* \geq \bar{t}_*^0$  is obtained in [5] on the basis of an investigation of the fracture front propagation in an arbitrary body by using a simple cumulative damage law (which is equivalent to the particular case  $\beta = 1$ ) which agrees completely with (29).

It is seen from relations (8), (11), (19), (30), (31) that the stress intensity distribution diagram in the case  $\beta = 1$  intersects an analogous steady creep diagram at a point with coordinate  $r = \bar{r}$  at any time  $0 < t \leq t_*$ , i.e., the stress intensity at this point is not redistributed during creep, but remains equal to its initial value

$$S_2(\bar{r}, t) = S_2^0(\bar{r}), \quad S_2(r, 0) = S_2^0(r).$$

The coordinate of this point is determined from (26), and is independent of the time. In particular, for a sphere

$$\frac{\bar{r}}{b} = \left[ \left( \frac{3g+n+6}{n+3} \right) \left( \frac{\lambda^{(n+3)/n} - 1}{\lambda^{(3g+n+6)/n} - 1} \right) \right]^{n/(3g+3)} (1 < n - g < 2); \quad (32)$$

and for a cylinder

$$\frac{\bar{r}}{b} = \left[ \frac{(g+2)(\lambda^{2/n} - 1)}{\lambda^{(2g+4)/n} - 1} \right]^{n/(2g+2)} (1 < n - g < 2). \quad (33)$$

It is seen that the coordinates (32) and (33) differ insignificantly from the corresponding coordinates for intersection of the elastic and steady distribution diagrams, and for  $\eta \rightarrow \infty$  agree exactly with the coordinates for intersection of the elastic stress intensity distribution with the ideal plastic distribution. In combination with (30) and (31), this result affords a possibility of involving an electronic computer (or using it minimally) to compute the stress-strain state of high-pressure vessels by means of (8) and (9) even in the case  $\beta \neq 1$  as an approximate estimate during design. The lower bound of the fracture time is determined from (29) or from the expression  $t_* \geq \bar{t}_*$  proposed in [5]. In combination with (30), (31) and (29), the relationships (8) and (9) yield the exact solution for  $\beta = 1$ .

#### LITERATURE CITED

1. Yu. N. Rabotnov, Creep of Structure Elements [in Russian], Nauka, Moscow (1966).
2. L. M. Kachanov, Theory of Creep [in Russian], Fizmatgiz, Moscow (1960).
3. Yu. N. Rabotnov, "On fracture because of creep," Prikl. Mekh. Tekh. Fiz., No. 2 (1963).
4. O. V. Sosnin, "On a variant of creep theory with hardening energy parameters," in: Mechanics of Deformable Bodies and Structures [in Russian], Mashinostroenie, Moscow (1975).
5. F. A. Leckie and D. R. Hayhurst, "Creep rupture of structures," Proc. R. Soc. London A, 340 (1974).

#### ST. VENANT PRINCIPLE FOR STRONGLY ANISOTROPIC ELASTIC MEDIA

Yu. A. Bogan

UDC 539.1

The presence of strong anisotropy in modern composites (consequently, large parameters are present in the generalized Hooke's law for the average stresses) results in limit models being characterized by the phenomenon of "propagation" of the stress state [1].

In this connection, the question occurs as to what degree does the St. Venant principle remain valid for media with inextensible fibers? As is shown below, exponentiality decreasing the potential strain energy with distance from the domain of self-equilibrated load application occurs [2] for media with inextensible fibers under definite conditions; however, it is hence generally impossible to make a deduction about the exponentiality of the damping with distance from the loaded section.

Therefore, the St. Venant principle must be formulated in a weakened, integral form without local estimates of the stress state of the structure for the application of the principle to media with inextensible fibers.

1. Without pinpointing any specific model of a linearly elastic composite, let us take the generalized Hooke's law relationship in the form

$$\sigma_{\xi} = A_{11}e_{\xi} + A_{12}e_{\eta}, \quad \sigma_{\eta} = A_{12}e_{\xi} + A_{22}e_{\eta}, \quad \tau_{\xi\eta} = G\gamma_{\xi\eta}, \quad (1.1)$$

where  $\xi = x \cos \alpha = y \sin \alpha$ ;  $\eta = -x \sin \alpha + y \cos \alpha$ ;  $0 \leq \alpha < \pi$  is some constant angle, and  $(x, y)$  are cartesian orthogonal coordinates. Let us put

$$\varepsilon^{-2} = A_{11}G^{-1}, \quad d_{12} = A_{12}G^{-1}, \quad d = A_{22}G^{-1}, \\ \bar{\sigma}_{\xi} = \sigma_{\xi} G^{-1}, \quad \bar{\sigma}_{\eta} = \sigma_{\eta} G^{-1}, \quad \bar{\tau}_{\xi\eta} = \tau_{\xi\eta} G^{-1}$$

Novosibirsk. Translated from Zhurnal Prikladnoi Mekhaniki i Tekhnicheskoi Fiziki, No. 2, pp. 164-169, March-April, 1980. Original article submitted June 28, 1979.